NANOSYSTEMS: PHYSICS, CHEMISTRY, MATHEMATICS, 2013, 4 (5), P. 648–656

DEPENDENCE OF QUANTUM YIELD OF UP-CONVERSION LUMINESCENCE ON THE COMPOSITION OF FLUORITE-TYPE SOLID SOLUTION $NaY_{1-x-y}Yb_xEr_yF_4$

D. S. Yasyrkina, S. V. Kuznetsov, A. V. Ryabova, D. V. Pominova,
V. V. Voronov, R. P. Ermakov, P. P. Fedorov

A. M. Prokhorov General Physics Institute, Russian Academy of Sciences,
38 Vavilov Street, Moscow, 119991, Russia

ppfedorov@yandex.ru

PACS 78.20-e

A study of the properties of polycrystalline fluorite-type $NaY_{1-x-y}Yb_xEr_yF_4$ solid solutions demonstrated that $NaY_{0.87}Yb_{0.10}Er_{0.03}F_4$ and $NaY_{0.885}Yb_{0.1}Er_{0.015}F_4$ samples produced up-conversion luminescence with 3.35% and 3.62% quantum yields, which were higher than quantum yields of the other $NaY_{1-x-y}Yb_xEr_yF_4$ samples. $NaY_{1-x-y}Yb_xEr_yF_4$ specimens were prepared by co-precipitation from aqueous solutions by drop-wise addition of rare earth nitrate solutions to aqueous sodium fluoride.

Keywords: fluorides, nanopowders, sodium, yttrium, up-conversion luminescence, quantum yield.

1. Introduction

At the present time, scientists are actively looking for materials that can efficiently transform infrared light to visible light by up-conversion for photodynamic cancer therapy (PDT) [1-3]. In order to satisfy the PDT strict requirements, these materials must have a high photochemical activity (i.e., they must effectively produce reactive oxygen species when excited); their particle size should be ca. 30–80 nm; their excitation should occur at the maximal transparency of human tissue; they should possess a specificity toward target tissues and low toxicity. Among the various substances that are used for photodynamic therapy (oxides, fluorides, CdSe-based quantum dots, etc.), Yb- and/or Er-doped $NaYF_4$ matrices maintain a special place, because of their unusually high up-conversion quantum yields [4-6].

Properties of these matrices stem from the features intrinsic to $NaYF_4$. According to the phase diagram of NaF-YF_3 [7] (Fig. 1), $NaYF_4$ exists in the form of two phases: a high-temperature non-stoichiometric cubic phase with fluorite structure (phase F) and a low-temperature hexagonal phase with Gagarinite-type structure (cubic phase F may be prepared in metastable state by low temperature synthesis [1]).

Researchers believe that the most promising up-converter matrix is the low-temperature hexagonal $NaYF_4$ phase, due to its high quantum yield values. This phase can be synthesized by various methods [1], but all of them require special conditions. We have shown [9] that it was possible to prepare hexagonal $NaYF_4$ at room temperature by co-precipitation from aqueous solutions in the presence of some structure-forming substances like polyethyleneimine (PEI), but the obtained products frequently were not thermally stable and were not suitable for fluorescence studies. Literature description of the aforementioned

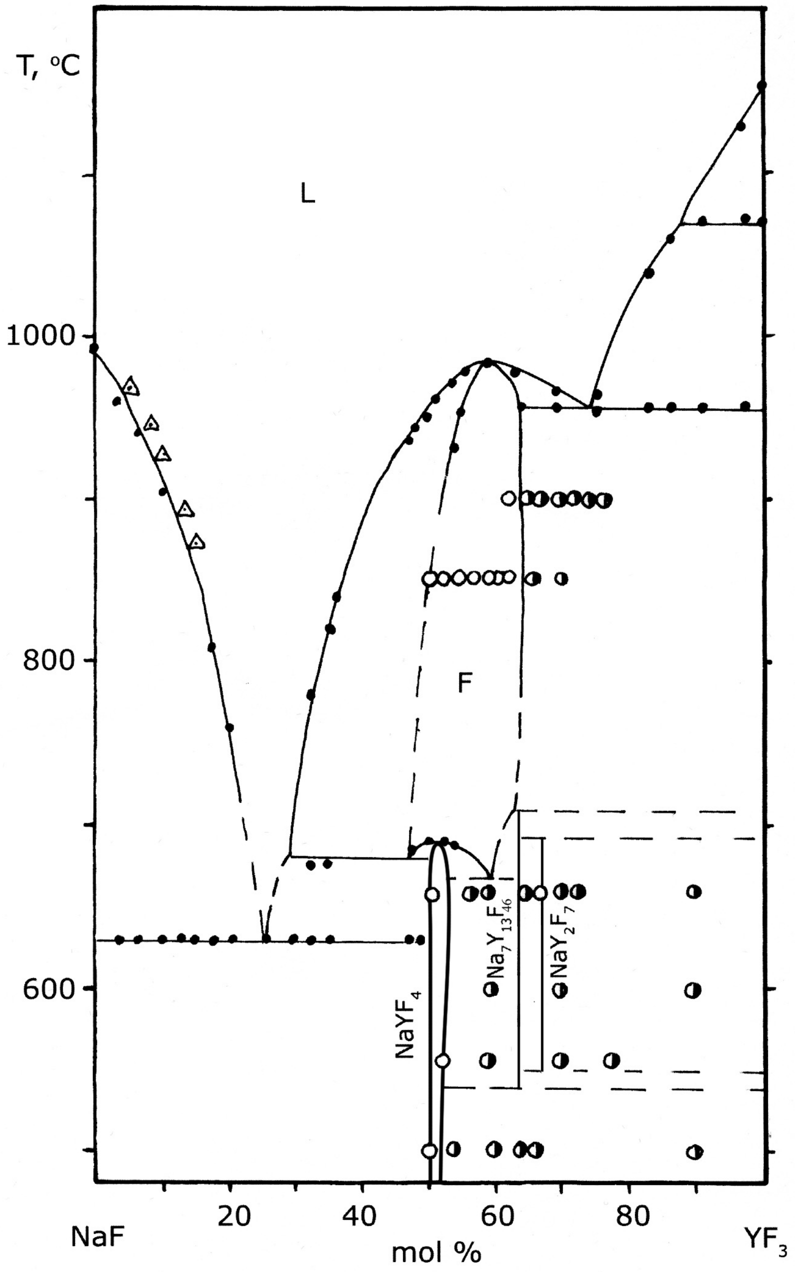

FIG. 1. NaF-YF$_3$ phase diagram [7, 8]: L — melt, F — cubic fluorite-type $Na_{0.5-x}Y_{0.5+x}F_{2+2x}$,

●, Δ — differential thermal analysis (DTA) data,
○ — single-phase samples,
◑ — two-phase samples (X-ray diffraction data)

doped $NaYF_4$ matrices is vast, but limited in its scope [4]. It should be noted that other researchers [1] focused their attention primarily on two compositions only, $NaYF_4$:Yb(20 mol. %):Er(2 mol. %) and $NaYF_4$:Yb(17 mol. %):Er(3 mo. 1%), without revealing the reasons for their choice. Also, various techniques were used to measure the quantum yields of their specimens as well as they prepared their samples by different methods [4]. As a result, the described optical materials possess different amounts of different impurities that seriously affect the obtained quantum yield data, and these circumstances make comparison of the existing literature data impossible.

Therefore, the aim of our study was a systematic research of the polycrystalline heat-resistant fluorite-type $NaY_{1-x-y}Yb_xEr_yF_4$ solid solutions, prepared by the same method, in order to find dopant concentrations which yielded the highest up-conversion quantum yields.

2. Experimental

We used 99.99 wt. % pure $Y(NO_3)_3{\cdot}6H_2O$, $Yb(NO_3)_3{\cdot}6H_2O$, $Er(NO_3)_3{\cdot}5H_2O$ (Lanhit, Moscow, Russia), NaF (99 wt. % pure) and double distilled water were used as starting materials. All experiments were carried out in a polypropylene reactor with polypropylene stirring bar and polypropylene solution dispensers at room temperature unless otherwise specified. Dropwise addition of the starting solutions was done under vigorous stirring. Phase compositions of the solid specimens were evaluated by X-ray diffraction (DRON-4M diffractometer; CuKα radiation; graphite monochromator). Calculations of the lattice parameters were done using Powder 2.0 software. We used NVision 40 workstation to record scanning electron microscopy (SEM) images of the formed nanoparticles.

Optical spectroscopy studies included the registration of up-conversion luminescence spectra at 400–900 nm and diffusely reflected excitation laser radiation, followed by calculation of the absolute quantum yields. We used our own assembly that included fiber optic LESA-01-BIOSPEC spectrometer (BIOSPEC, Russia) with a modified integrating sphere (Avantes, Netherlands) and Y-shaped fiber catheter (974 nm laser excitation wavelength; 1 W laser power output; UnoMomento processing software) [10]. The spectrometer was calibrated with LEDs of different wavelengths and known outputs as well as with LabMax®-TO power meter (Coherent, USA). Powder samples were placed between two cover slips, which were then fastened together and placed inside the integrating sphere. The scattered radiation was captured by the optical fibers connected to the spectrometer.

The quantum yield (QY) of the produced up-conversion luminescence was calculated [9] according to equation (1):

$$QY = \frac{P^{Sample}_{emitted}}{P^{Sample}_{974\_absorbed}} = \frac{P^{Sample}_{emitted}}{P^{Reference}_{974\_scattered} - P^{Sample}_{974\_scattered}}\quad , \tag{1}$$

where:

— $P^{Sample}_{emitted}$ is power of radiation emitted by the sample and

— $P^{Sample}_{974\_absorbed}$ is the output power of 974 nm laser, absorbed by the sample.

The latter is equal to the difference between:

— $P^{Reference}_{974\_scattered}$ - the power of the scattered radiation of the reference specimen and

— $P^{Sample}_{974\_scattered}$ - the power of the scattered radiation of the studied sample.

Reference samples were chosen among specimens containing no activator ions (e.g., intrinsic $NaYF_4$) in order to enhance the accuracy of our measurements.

3. Sample preparation

Synthesis of fluoride nanopowders was done by co-precipitation from aqueous solution described in detail in [11, 12]. We used aqueous rare earth nitrates and sodium fluoride solutions of the same concentrations (0.35 M). Yttrium and dopant rare earth solutions were premixed before aqueous NaF was added to them under vigorous stirring. All experiments were carried out with 10-fold excess of NaF (calculated for $NaRF_4$ stoichiometry). Precipitates were separated from their mother solutions by decanting. Collected precipitates were washed twice with double distilled water and dried at 35 ° C under air. Calcination of the obtained samples was performed in an oven at 600 ° C for 1 hour at a heating rate of 10 ° C/min. In some cases, we used an Eppendorf 5804 centrifuge to separate precipitates from the mother liquors in order to reduce time of synthetic experiments.

4. Results and Discussion

Samples of $NaY_{1-x-y}Yb_xEr_yF_4$ were synthesized with an Yb content (x) which varied from 2 to 90 mol. %, and an Er content (y) that varied from 0.5 to 20 mol. %. According to X-ray analysis, all samples contained only one fluorite-type phase (Table 1). A typical X-ray diffraction pattern of one of the synthesized samples (nominal composition $NaY_{0.6}Yb_{0.3}Er_{0.1}F_4$) is shown in Fig. 2.

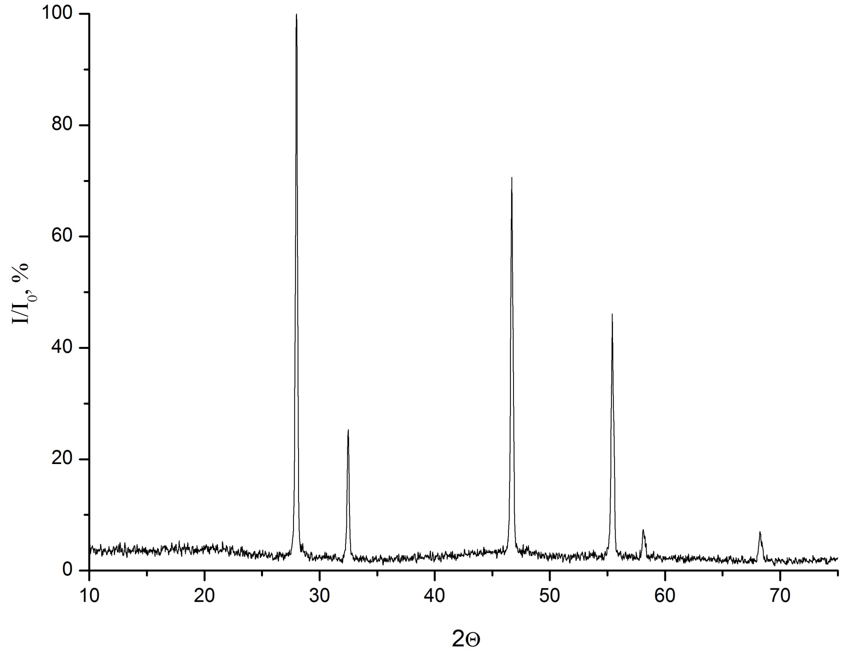

FIG. 2. Typical X-ray diffraction pattern of fluorite-type $NaY_{0.6}Yb_{0.3}Er_{0.1}F_4$ sample

These single phase specimens contained 50–90 nm particles that formed 200–350 nm agglomerates (Fig. 3). The size of the latter is higher than the required particle size for photodynamic therapy (30–80 nm), but breaking up the agglomerates and dispersion of the individual particles were left outside of the scope of the present paper.

We evaluated $NaY_{1-x-y}Yb_xEr_yF_4$ sample compositions with the use of correlation (2) between lattice parameter of $Na_{0.5-x}R_{0.5+x}F_{2+2x}$ fluorite-type solid solutions and content of the rare earth ion [13]:

$$a = 5.398 + (6.7238 \times r^{cp} - 7.259) \times (x + 0.13), \tag{2}$$

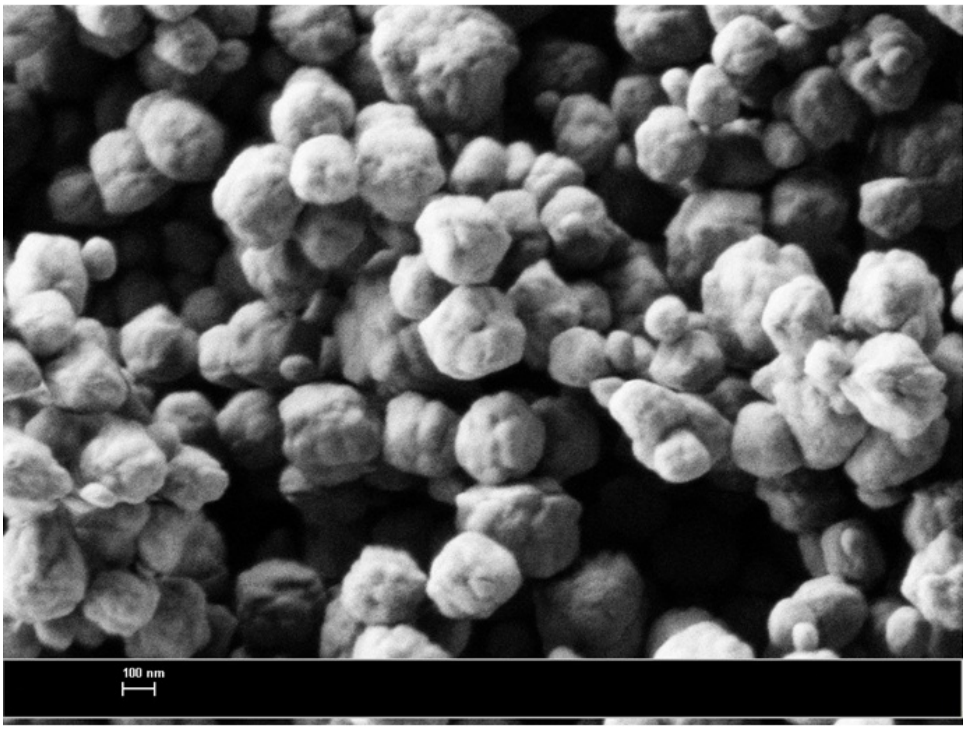

FIG. 3. Typical SEM image of the single phase sample with total $NaY_{0.6}Yb_{0.3}Er_{0.1}F_4$ composition

where a is a cubic unit cell lattice parameter (Å) and r is the effective RE^{3+} ionic radius.

Because our samples were doped with ytterbium and erbium, we had to adjust the effective ionic radius of the rare-earth cation according to the following formula:

$$r_{cp} = X_Y * r_Y + X_{Yb} * r_{Yb} + X_{Er} * r_{Er}, \tag{3}$$

where $r_Y = 1.159$ Å, $r_{Yb} = 1.125$ Å, and $r_{Er} = 1.144$ Å are ionic radii of the corresponding elements [13], and X_Y, X_{Yb} and X_{Er} are their molar parts.

Estimated compositions of synthesized samples $Na_{0.5-x}R_{0.5+x}F_{2+2x}$ are given in Table 1.

The quantum yield of up-conversion luminescence in the visible range of the spectrum (QY) was calculated by summarizing the integrated luminescence decay intensities corresponding to the following Er^{3+} transitions: $^2P_{3/2} \rightarrow ^4I_{11/2}$ at 480 nm; $^2H_{11/2} \rightarrow ^4I_{15/2}$ at 525 nm; $^4S_{3/2} \rightarrow ^4I_{15/2}$ at 545 nm; and $^4F_{9/2} \rightarrow ^4I_{15/2}$ at 665 nm (1 W/cm^2 the pump power density). The quantum yields of the other Er^{3+} transitions in the red region of the spectrum ($^4F_{9/2} \rightarrow ^4I_{15/2}$ at 665 nm) (QY_r) as well as in the green region of the spectrum ($^2H_{11/2} \rightarrow ^4I_{15/2}$ at 525 nm and $^4S_{3/2} \rightarrow ^4I_{15/2}$ at 545 nm) (QY_g) and $f_{r/g}$ factor value, which characterizes the ratio of the intensities of the decay up-conversion luminescence in the red and green areas, were also accounted for.

The results of our studies for the up-conversion luminescence quantum yields as a function of ytterbium and erbium dopant concentrations are presented in Table 2 and Figs. 4(a,b).

The intensity of up-conversion luminescence was proportional to the amount of absorbed IR photons [14], but it exhibited a nonlinear dependency from the pump power density: quantum yields were lower at 800 mW/cm^2 pump density than at 1000 mW/cm^2 (Table 2).

TABLE 1. The lattice parameters of fluorite-type $NaY_{1-x-y}Yb_xEr_yF_4$ samples, their estimated compositions and quantum yields

Samples	Sample nominal composition	Cubic lattice parameter a, Å	Calculated composition, $Na_{0.5-x}R_{0.5+x}F_{2+2x}$	QY, %	QY_r %	QY_g %	$f_{r/g}$
F391	$NaY_{0.80}Yb_{0.17}Er_{0.03}F_4$	5.483(8)	$Na_{0.457}R_{0.543}F_{2.086}$	0.32	0.29	0.03	2.36
F393	$NaYb_{0.90}Er_{0.10}F_4$	5.448(1)	$Na_{0.466}R_{0.534}F_{2.068}$	0.02	0.02	< 0.01	4.11
F394	$NaY_{0.60}Yb_{0.30}Er_{0.10}F_4$	5.474(1)	$Na_{0.463}R_{0.537}F_{2.074}$	0.07	0.06	0.01	1.27
F398	$NaY_{0.20}Yb_{0.60}Er_{0.20}F_4$	5.454(1)	$Na_{0.476}R_{0.524}F_{2.048}$	0.01	0.01	< 0.01	2.28
F406	$NaY_{0.70}Yb_{0.10}Er_{0.2}F_4$	5.4861(6)	$Na_{0.477}R_{0.523}F_{2.046}$	0.05	0.05	< 0.01	2.25
F407	$NaY_{0.80}Yb_{0.10}Er_{0.10}F_4$	5.438(1)	$Na_{0.55}R_{0.45}F_{1.9}$	0.08	0.07	0.01	2.08
F442	$NaY_{0.63}Yb_{0.17}Er_{0.20}F_4$	5.474(2)	$Na_{0.459}R_{0.541}F_{2.082}$	0.22	0.19	0.03	1.49
F443	$NaY_{0.73}Yb_{0.17}Er_{0.10}F_4$	5.4840(4)	$Na_{0.451}R_{0.549}F_{2.098}$	0.04	0.04	< 0.01	2.10
F461	$NaY_{0.50}Yb_{0.30}Er_{0.20}F_4$	5.474(1)	$Na_{0.459}R_{0.518}F_{2.082}$	0.05	0.05	< 0.01	2.80
F462	$NaY_{0.67}Yb_{0.30}Er_{0.03}F_4$	5.464(3)	$Na_{0.487}R_{0.513}F_{2.026}$	0.22	0.21	0.01	3.89
F465	$NaY_{0.685}Yb_{0.30}Er_{0.015}F_4$	5.463(1)	$Na_{0.49}R_{0.51}F_{2.02}$	0.41	0.30	0.11	0.69
F471	$NaY_{0.37}Yb_{0.60}Er_{0.03}F_4$	5.4642(5)	$Na_{0.462}R_{0.538}F_{2.076}$	0.11	0.11	< 0.01	5.86
F472	$NaY_{0.385}Yb_{0.60}Er_{0.015}F_4$	5.4632(8)	$Na_{0.465}R_{0.535}F_{2.07}$	0.04	0.04	< 0.01	2.94
F473	$NaY_{0.07}Yb_{0.90}Er_{0.03}F_4$	5.446(1)	$Na_{0.482}R_{0.518}F_{2.036}$	0.07	0.07	< 0.01	5.06
F474	$NaY_{0.085}Yb_{0.90}Er_{0.015}F_4$	5.446(1)	$Na_{0.489}R_{0.511}F_{2.022}$	0.07	0.07	< 0.01	6.18
F647	$NaY_{0.95}Yb_{0.02}Er_{0.03}F_4$	5.493(7)	$Na_{0.541}R_{0.459}F_{1.918}$	0.31	0.16	0.15	0.28
F648	$NaY_{0.935}Yb_{0.05}Er_{0.015}F_4$	5.485(2)	$Na_{0.357}R_{0.643}F_{2.286}$	1.41	0.70	0.71	0.25
F685	$NaY_{0.77}Yb_{0.2}Er_{0.03}F_4$	5.476(2)	$Na_{0.47}R_{0.53}F_{2.06}$	1.53	1.11	0.42	0.67
F693	$NaY_{0.87}Yb_{0.10}Er_{0.03}F_4$	5.487(6)	$Na_{0.454}R_{0.546}F_{2.092}$	3.35	2.73	0.62	1.12
F702	$NaY_{0.885}Yb_{0.10}Er_{0.015}F_4$	5.481(2)	$Na_{0.466}R_{0.534}F_{2.068}$	3.62	2.48	1.14	0.55
F704	$NaY_{0.815}Yb_{0.17}Er_{0.015}F_4$	5.499(2)	$Na_{0.431}R_{0.569}F_{2.138}$	2.03	1.62	0.41	1.01
F740	$NaY_{0.895}Yb_{0.1}Er_{0.005}F_4$	5.4887(8)	$Na_{0,452}R_{0,548}F_{2,096}$	0.99	0.61	0.38	0.41
F741	$NaY_{0.825}Yb_{0.17}Er_{0.005}F_4$	5.4860(7)	$Na_{0,452}R_{0,548}F_{2,096}$	1.18	0.77	0.41	0.47
F743	$NaY_{0.695}Yb_{0.3}Er_{0.005}F_4$	5.4800(7)	$Na_{0,454}R_{0,546}F_{2,092}$	1.79	1.30	0.49	0.67
F744	$NaY_{0.395}Yb_{0.6}Er_{0.005}F_4$	5.464(1)	$Na_{0,463}R_{0,537}F_{2,074}$	0.56	0.51	0.05	2.55
F745	$NaY_{0.095}Yb_{0.9}Er_{0.005}F_4$	5.451(1)	$Na_{0,438}R_{0,562}F_{2,124}$	0.25	0.24	0.01	4.24

TABLE 2. Sample quantum yield at 800 mW/cm^2 and 1000 mW/cm^2 pump power

Samples	Sample nominal composition	Capacity, mW/cm^2	QY, %	$f_{r/g}$	QY_r, %	QY_g, %
F693	$NaY_{0.87}Yb_{0.10}Er_{0.03}F_4$	800	1.10	1.38	0.93	0.17
		1000	3.35	1.12	2.73	0.62
F685	$NaY_{0.77}Yb_{0.2}Er_{0.03}F_4$	800	1.22	0.75	0.91	0.31
		1000	1.53	0.67	1.11	0.42
F702	$NaY_{0.885}Yb_{0.10}Er_{0.015}F_4$	800	2.21	0.55	1.51	0.70
		1000	3.64	0.55	2.48	1.14
F704	$NaY_{0.815}Yb_{0.17}Er_{0.015}F_4$	800	1.74	0.97	1.38	0.36
		1000	2.03	1.01	1.62	0.41

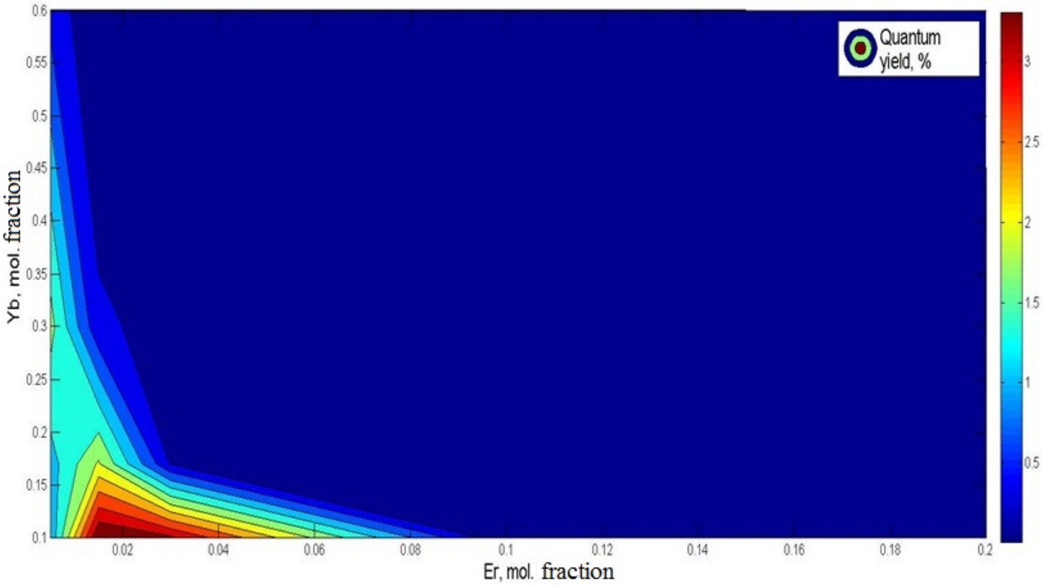

(a)

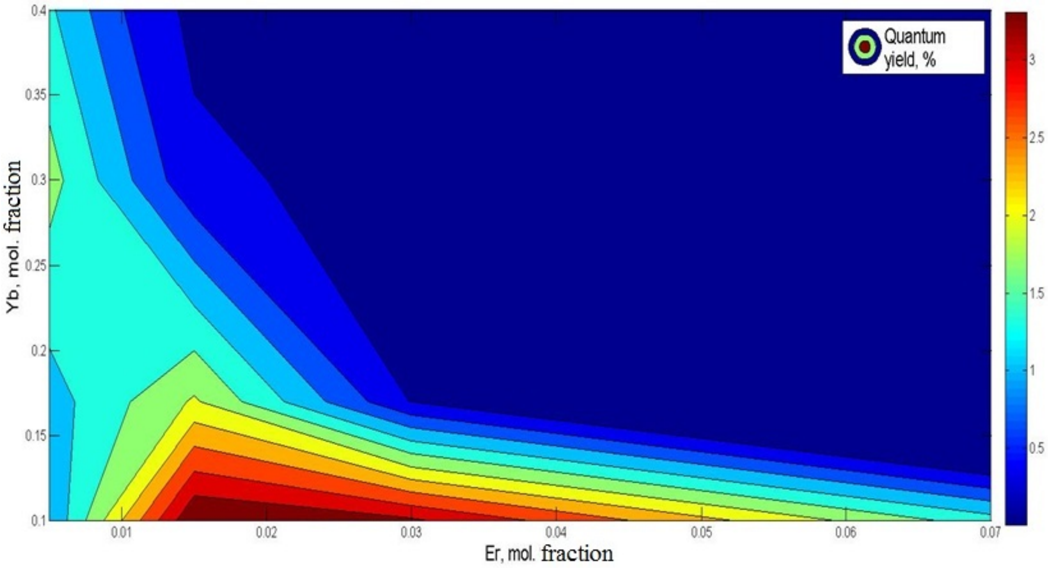

(b)

FIG. 4. The color-coded absolute quantum yields of the up-conversion luminescence $NaY_{1-x-y}Yb_xEr_yF_4$ samples vs. doping Yb and Er concentrations: 0.1–0.6 mol. fraction Yb and 0–0.2 mol. fraction Er (a); 0.1–0.4 mol. fraction Yb and 0.005–0.07 mol. fraction Er (b)

Fig. 4 data clearly indicated the composition area with the highest quantum yields correspond to the samples containing 0.5–3 mol. % Er and 10–20 mol. % Yb as well as about 0.15 mol. % Er and about 10 mol. % Yb. $NaY_{0.87}Yb_{0.10}Er_{0.03}F_4$ (3.35 %) and $NaY_{0.885}Yb_{0.1}Er_{0.015}F_4$ (3.62 %) specimens demonstrated the highest quantum yields achieved during our experiments. Their composition was significantly different from the compositions of the samples described in the literature [1]. It is very hard to compare our results with previous data [1, 4], for, as we have already mentioned above, different researchers utilized different synthetic methods (including different conditions of incongruent crystallization of the samples) and, therefore, impurity content and sample compositions were also different. However, it is worth noting that some authors [15, 16] reported a quantum yield decrease with decreased particle size for sub-micron crystals, whereas the quantum yields of their micron-sized agglomerates were the same as those obtained for bulk samples. All of their samples [15, 16] did not provide up-conversion quantum yields above 3.5% while still being unsuitable for photodynamic therapy because of their large size. In the present study, we achieved quantum yields above 3% using much smaller 50–90 nm particles. Further study of Yb/Er-doped $NaYF_4$ samples as prospective optical materials for use in photodynamic therapy are ongoing, and results will be reported soon.

5. Conclusions

$NaY_{1-x-y}Yb_xEr_yF_4$ specimens were prepared by co-precipitation from aqueous solutions by dropwise addition of rare earth nitrate solutions to aqueous sodium fluoride. Study of the properties of polycrystalline fluorite-type $NaY_{1-x-y}Yb_xEr_yF_4$ solid solutions demonstrated that $NaY_{0.87}Yb_{0.10}Er_{0.03}F_4$ and $NaY_{0.885}Yb_{0.1}Er_{0.015}F_4$ samples produced up-conversion luminescence with 3.35% and 3.62% quantum yields, which were higher than the quantum yields of the other $NaY_{1-x-y}Yb_xEr_yF_4$ samples. The 50–90 nm particle size of the synthesized $NaY_{1-x-y}Yb_xEr_yF_4$ specimens makes them useful for photodynamic therapy once a practical method for the dispersion of their 200–350 nm agglomerates is found.

Acknowledgements

This work was supported by the grants of the Federal Program “Scientific and scientific-pedagogical personnel of innovative Russia” (State contract N 14.740.12.1343), RFBR (12-02-00851/a, N 12-02-12080-ofi-m, 13-02-12162 ofi-m) and a grant of the leading scientific schools (NSH-341.2012.2). Authors are very grateful to A. Baranchikov for his assistance in scanning electron microscopy studies and A. I. Popov and E. Chernova for their help in the manuscript preparation.

References

[1] P.P. Fedorov, A.A. Luginina, S.V. Kuznetsov, and V.V. Osiko. Nanofluorides. *J. Fluorine Chem.*, **132**, P. 1012–1039 (2011).

[2] P. Zhang, W. Steelant, M. Kumar, M. Scholfield. Versatile photosensitizers for photodynamic therapy at infrared excitation. *J. Am. Chem. Soc.*, **129**, P. 4526–45257 (2007).

[3] D.K. Chatterjee, L. Sh. Fong, and Y. Zhang. Nanoparticle photodynamic therapy PDT. *Advanced Drug Delivery Reviews.*, **60**, P. 1627–1637 (2008).

[4] M. Haase and H. Schafer. Upconverting Nanoparticles. *Angew. Chem. Int. Ed.*, **50**, P. 5808-5829 (2011).

[5] F. Auzel. Upconversion and anti-stokes processes with f and d ions in solids. *Chem Rev.*, **104**, P. 139–173 (2004).

[6] V.V. Ovsyankin, P.P. Feofilov. Mechanism of summation of electronic excitations in activated crystals. *JETP Lett.*, **3**, P. 322–323 (1966).

[7] P.P. Fedorov. Systems of alkali and rare-earth metal fluorides. *Russian J. Inorg. Chem.*, **44**, P. 1703–1727 (1999).

[8] P.P. Fedorov, B.P. Sobolev, S.F. Belov. Fusibility diagram of the system NaF-YF_3, and the cross-section $Na_{0.4}Y_{0.6}F_{2.2}$-YOF. *Inorg. Mater.*, **15**(5), P. 640–643 (1979).

[9] S.V. Kuznetsov, A.V. Ryabova, D.S. Los‘, P.P. Fedorov, V.V. Voronov, R.P. Ermakov, V.B. Loshchenov, V.V. Volkov, A.E. Baranchikov, V.V. Osiko. Synthesis and luminescent characteristics of submicron powders on the basis of sodium and yttrium fluorides doped with rare earth elements. *Nanotechnologies in Russia*, **7**, P. 615–628 (2012).

[10] A.V. Ryabova, D.V. Pominova, V.A. Krut'ko, M.G. Komova, V.B. Loschenov. Spectroscopic research of upconversion nanomaterials based on complex oxide compounds doped with rare-earth ion pairs: benefit for cancer diagnostics by upconversion fluorescence and radio sensitive methods. *Photon Lasers Med* (2013). DOI 10.1515/plm-2013-0013.

[11] P.P. Fedorov, S.V. Kuznetsov, V.V. Voronov, I.V. Yarotskaya, V.V. Arbenina. Soft chemical synthesis of $NaYF_4$ nanopowders. *Russian J. Inorg. Chem.*, **53**, P. 1681–1685 (2008).

[12] D.S. Yasyrkina, S.V. Kuznetsov, P.P. Fedorov, V.V. Voronov, R.P. Ermakov, A.V. Ryabova, et al. Effect of the pH on the formation of $NaYF_4$:Yb:Er nanopowders by co-crystallization in presence of polyethyleneimine. *J. Fluorine Chem.*, accepted for publication.

[13] P.P. Fedorov, V.B. Alexandrov, O.S. Bondareva, I.I. Buchinskaya, M.D. Val'covskii, and B.P. Sobolev. Concentration dependences of the unit-cell parameters of nonstoichiometric fluorite-type phases $Na_{0,5-x}R_{0,5+x}F_{2+2x}$ (R = Rare-earth elements). *Crystallography Reports.*, **46**, P. 239–245 (2001).

[14] M. Pollnau, D. R. Gamelin, S. R. Luthi, H. U. Gudel, M. P. Hehlen. Power dependence of upconversion luminescence in lanthanide and transition-metal-ion systems. *Phys. Rev. B*, **61**, P. 3337–3346 (2000).

[15] D.O. Faulkner, S. Petrov, D.D. Perovic, N.P. Kherani, G.A. Ozin. Absolute quantum yields in $NaYF_4$:Er,Yb upconverters – synthesis temperature and power dependence. *J. Mater. Chem.*, **22**, P. 24330–24334 (2012).

[16] J-Ch. Boyer and Fr. van Veggel. Absolute quantum yield measurements of colloidal $NaYF_4$: Er^{3+},Yb^{3+} upconverting nanoparticles. *Nanoscale*, **2**, P. 1417–1419 (2010).